An XPS Study of the Interaction of Ultrathin Cu Films with Pd(111)

G. Liu, T. P. St. Clair, and D. W. Goodman*

Department of Chemistry, Texas A&M University, P.O. Box 30012, College Station, Texas 77842-3012

Received: June 7, 1999; In Final Form: August 17, 1999

The interaction of ultrathin Cu films with Pd(111) was studied by X-ray photoelectron spectroscopy (XPS). The effects of Cu coverage and annealing temperature were investigated. The XPS data show that at room temperature Cu grows on Pd(111) layer-by-layer without alloying. Furthermore, Cu $2p_{3/2}$ core-level shifts as a function of film thickness indicate that the Cu−Pd interactions perturb the electronic properties of two to three layers of Cu atoms. The Cu $2p_{3/2}$ binding energy of a Cu monolayer at room temperature was shifted by −0.47 eV relative to a Cu(100) surface. XPS core-level shifts demonstrate that by annealing to temperatures higher than 450 K the Cu overlayer alloys with the Pd substrate. After annealing to 900 K, the Cu $2p_{3/2}$ binding energy for 1.0 ML Cu coverage was observed to shift −0.49 eV relative to that of 1 ML Cu/Pd(111). The XPS binding energy shifts are discussed in terms of both initial and final state effects.

1. Introduction

Bimetallic surfaces possess novel physical and chemical properties and consequently have been studied extensively over the last 10 years.[1−5] The focus of these studies has been to better understand the unique function of these surfaces in heterogeneous catalysis. Pd and Cu are two metals often paired because their interaction typically results in an improved heterogeneous catalyst. Pd−Cu catalysts are active for a number of reactions, including CO and alkene oxidation;[6,7] CO, benzene, toluene, and 1,3-butadiene hydrogenation;[8−11] and ethanol decomposition.[11] Pd−Cu alloys are also promising catalysts for NO reduction with CO. It has been reported that Pd is more active for CO oxidation[12] while Cu is more active for NO dissociation.[13] Thus, both components are believed to work together to catalyze the CO−NO reaction.

The heteroepitaxial growth of Cu on transition metal surfaces such as Re(0001), Ru(0001), Pt(111), and Rh(100)[1−3] has been studied to explore the perturbed electronic and chemical properties of the bimetallic surface compared to the corresponding monometallic single-crystal surfaces. For example, electronic structures have been correlated with catalytic properties by comparing CO chemisorption energies to surface core-level shifts (SCLS)[1] obtained by XPS. With respect to the measured binding energy of Cu(100) (a convenient energy reference), Cu $2p_{3/2}$ SCLS were found (for a pseudomorfic Cu monolayer) to be +0.02 eV on Re(0001), −0.13 eV on Ru(0001), −0.27 eV on Pt(111), and −0.43 eV on Rh(100).[1] Furthermore, a correlation between the strength of the Cu−CO bond and the magnitude of the negative SCLS has been well-established.[1]

The growth of Pd on Cu surfaces has also been investigated recently. A Volmer−Weber (VW), or island, growth mode is expected because the Pd surface free energy (2.05 J m^{-2}) is larger than the sum of the Cu surface free energy (1.85 J m^{-2}) and the interface free energy (0.01 J m^{-2}).[14] However, STM images show that, for submonolayer Pd coverages on Cu surfaces, substitutional surface and subsurface alloying occurs. For example, at room temperature, Pd deposited on Cu(100)[15] and Cu(110)[16] alloys into the first Cu surface layer at submonolayer coverages. Upon alloying, Cu atoms form islands on the surface. In the case of Pd/Cu(111),[17] a surface alloy was only observed after annealing to ∼430 K. With respect to electronic perturbation studies, Pope et al.[18] reported that, in alloys formed by Pd deposition on Cu(100), the Pd and Cu core-level binding energies exhibit positive and negative shifts, respectively. Depending on the initial Pd coverage, a c(2 × 2) and a p4g interfacial alloy structure were observed, along with other disordered alloys. Thus, in terms of both geometric and electronic effects, Pd deposition on Cu substrates has been characterized.

The behavior of Cu films on Pd surfaces is quite different from that of Pd on Cu surfaces. Despite the rather large structural misfit (7%) between Pd (the nearest neighbor distance is 2.75 Å)[19] and Cu (the nearest neighbor distance is 2.56 Å),[20] layer-by-layer or Frank−van der Merwe (FV) growth was observed at 300 K for Cu/Pd(100),[21] Cu/Pd(110),[22] and Cu/Pd(111).[23] Moreover, theoretical calculations demonstrate that the Pd−Cu bond is stronger than the Pd−Pd and Cu−Cu bonds,[24] consistent with layer-by-layer growth.

In addition to potential industrial catalytic applications, Pd−Cu alloys have also been used as model photoemission systems.[25−28] These studies have attempted to address the interplay between initial state and final state effects, which ultimately determine the core-level changes of Cu and Pd.

In this paper, XPS results of Cu thin films deposited on Pd(111) are presented. The surface electronic structures are probed as a function of Cu coverage and annealing temperature by examining core-level shifts determined by XPS. Of particular interest is the electronic structure differences between overlayer and alloy cases for Cu on Pd(111).

2. Experimental Section

The experiments were carried out in a conventional ultrahigh vacuum (UHV) chamber, described in detail previously,[29] with a base pressure of ∼5 × 10^{-10} Torr. The system consists of two interconnected chambers, one for sample treatment and temperature-programmed desorption (TPD), and the other for electron spectroscopy using a Kratos XSA M800 hemispherical electron energy analyzer and a twin-anode X-ray gun (unmono-

* To whom correspondence should be addressed.

10.1021/jp991843j CCC: $18.00
Published on Web 09/16/1999

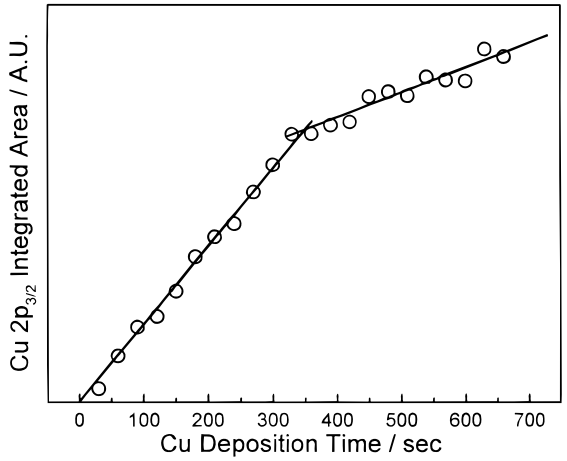

Figure 1. Variation of Cu $2p_{3/2}$ intensity as a function of Cu deposition time on Pd(111) at room temperature.

chromatized Mg Kα radiation was used for this study). XPS data is recorded at an electron takeoff angle of 30° with respect to the sample normal to enhance surface sensitivity. The spectrometer was operated in a fixed-analyzer transition mode with a pass energy of 65 eV. The core electron binding energies were calibrated with respect to clean Cu and Au surfaces.

The Pd(111) sample was polished with 1 μm diamond paste and 0.05 μm alumina following standard polishing procedures. The Pd(111) single crystal was mounted on tantalum leads and could be heated resistively. The crystal temperature was monitored with a W−5%Re/W−26%Re thermocouple spot-welded to the edge of the crystal. The sample was then cleaned in a vacuum by several cycles of argon ion bombardment followed by annealing to 800−900 K for 10 min until no contamination could be detected by XPS. The Cu source consisted of a high-purity Cu wire (99.997%, Johnson Matthew Chemical Limited) wrapped around a tantalum filament that could be heated resistively. The Cu source was extensively outgassed prior to use.

3. Results

The Cu coverage (film thickness) was calibrated by depositing incremental amounts of Cu on clean Pd(111) at room temperature and monitoring the XPS Cu 2p photoemission peaks between each dose. Figure 1 shows the Cu $2p_{3/2}$ integrated areas as a function of Cu deposition time. The Cu $2p_{3/2}$ peak areas increase linearly with evaporation time, with a marked slope change at ∼340 s. This change in slope is taken to indicate the completion of the first Cu monolayer. The linear increase in the Cu $2p_{3/2}$ integrated area with increasing coverage indicates that the first and second monolayers grow by forming two-dimensional (2D) islands.[30] Given that both the first and second monolayers form 2D islands, the growth mode for Cu/Pd(111) is consistent with layer-by-layer or Frank−van der Merwe (FM).

Figure 2 shows representative spectra of the Cu $2p_{3/2}$ and Pd($M_{4,5}VV$) regions for increasing Cu coverage deposited on Pd(111) at room temperature. The Cu $2p_{3/2}$ peak shifts from a binding energy of 931.96 eV at 0.5 and 1.0 ML coverages to a binding energy of 932.60 eV at both 10 and 20 ML (not shown). The Pd($M_{4,5}VV$) X-ray induced region shows a decrease in the Pd(M_5VV) to Pd(M_4VV) intensity ratio and a shift by +0.3 eV with increasing Cu coverage. The effect of Cu coverage on the Cu $2p_{3/2}$ peak positions is better illustrated in Figure 3, where the Cu $2p_{3/2}$ BE is plotted as a function of Cu coverage. Coverages less than 1 ML Cu resulted in no measurable shift in peak position from 931.96 eV. This result is consistent with

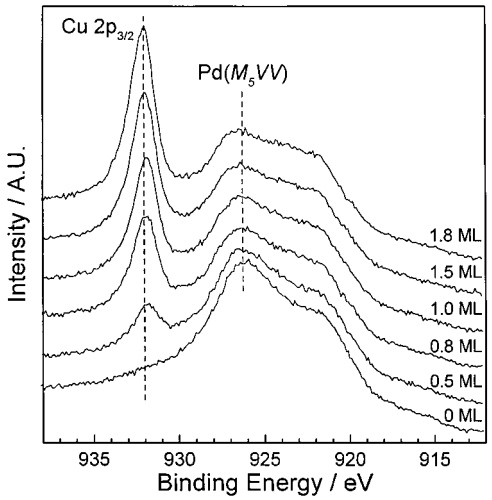

Figure 2. Effect of Cu coverage on the Cu $2p_{3/2}$ and Pd($M_{4,5}VV$) features.

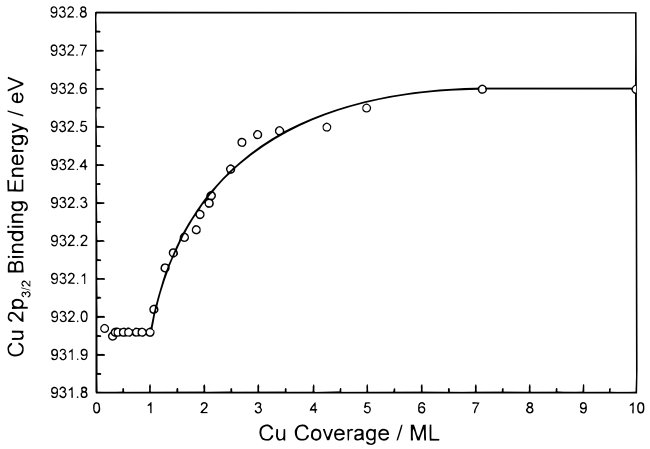

Figure 3. Plot of Cu $2p_{3/2}$ XPS binding energy of Cu/Pd(111) as a function of Cu coverage (film thickness).

the formation of Cu 2D islands on the Pd(111) surface and supported the data of Figure 1. Submonolayer coverages of Cu on other transition metal surfaces such as Ru(0001), and Rh(100)[31] also exhibit similar core-level shifts. At coverages greater than 1 ML, the Cu $2p_{3/2}$ peak position increases to 932.55 eV at ∼5 ML. Coverages >5 ML show no further significant changes in peak position, indicating that only short-range electronic interactions between copper and Pd(111) are observed.

Figure 4 illustrates the effect of Cu coverage on the Pd 3d photoemission peaks. It should be noted that the Pd $3d_{5/2}$ peak overlaps with the Cu(L_3VV) Auger transition, complicating the interpretation of any changes associated with increasing Cu coverage. The Pd $3d_{3/2}$ peak position shifts slightly with increasing Cu coverage, for example, by +0.1 eV at 1.0 ML. The intensity and peak width of the Pd $3d_{3/2}$ feature decreases with increasing Cu coverage, while the Pd $3d_{5/2}$/Cu(L_3VV) overlap displays no significant changes due to the simultaneous Pd $3d_{5/2}$ peak decrease and Cu(L_3VV) peak increase. The small Pd $3d_{3/2}$ shift is attributed to the loss of the Pd(111) surface layer with Cu wetting.[32]

Submonolayer Cu films on Pd(111) were annealed, and the resulting core-level shifts were monitored to investigate the temperature dependence of Cu−Pd alloy formation and the resulting electronic effects, as well as to compare the electronic structure of Cu overlayers on Pd(111) with that of Cu−Pd alloys. For these experiments, the Cu films were vapor deposited at room temperature, and the spectra were collected at room

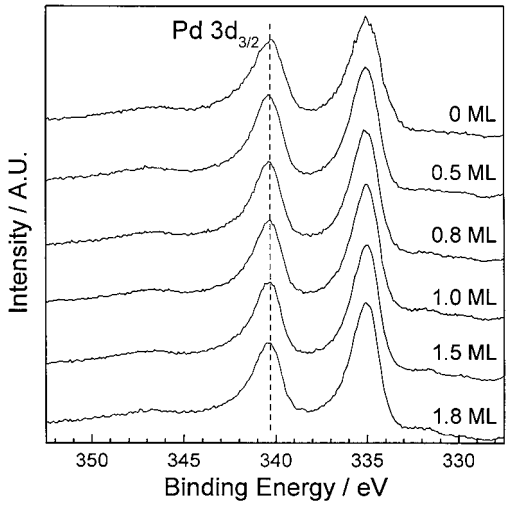

Figure 4. Effect of Cu coverage on the Pd $3d_{3/2}$ and Pd $3d_{5/2}$ XPS peaks.

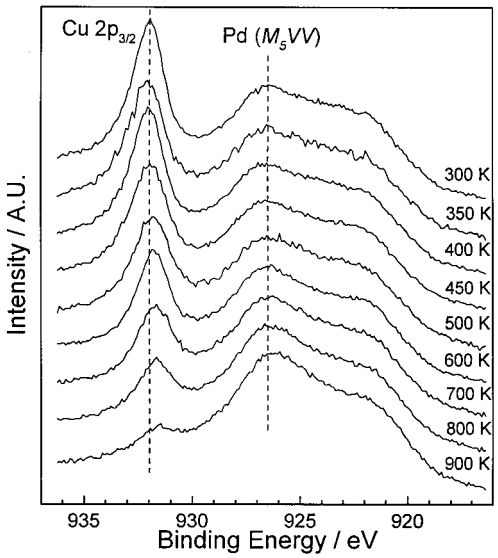

Figure 5. Annealing temperature effect on the Cu $2p_{3/2}$ and Pd($M_{4,5}VV$) features for 1 ML Cu/Pd(111).

temperature after annealing the sample at the specified temperature for 1 min. Figure 5 shows the effect of annealing on the Cu $2p_{3/2}$ and Pd(M_5VV) features for 1.0 ML Cu/Pd(111). Annealing to 500 K shifted the Cu $2p_{3/2}$ peak by −0.20 eV as compared to the peak position at 300 K. A maximum shift of −0.49 eV was observed by annealing to temperatures of 800 K or higher. The Pd(M_5VV) feature shifted −0.2 eV from 300 to 900 K, and the line shape gradually transformed to approximately that of the clean Pd surface by 900 K.

The Cu $2p_{3/2}$ peak intensity decreased with annealing temperature, particularly above 700 K, until at 900 K the intensity was 5% of the intensity at 300 K. This decrease with annealing temperature indicates either diffusion of Cu into the Pd bulk or Cu desorption. Thermal desorption experiments detected no Cu desorption from the Pd(111) surface (not shown), so the disappearance of Cu signal is attributed to Cu diffusion into the Pd(111) bulk. The negative CLS cannot be due to decreasing Cu coverage because no core-level shifts were observed for coverages below 1 ML (see Figure 3). Thus, the negative CLS that are observed upon annealing to T larger than 450 K are attributed to alloy formation (denoted $Pd_{1-x}Cu_x$/Pd(111)). The temperature required for alloy formation is similar to that

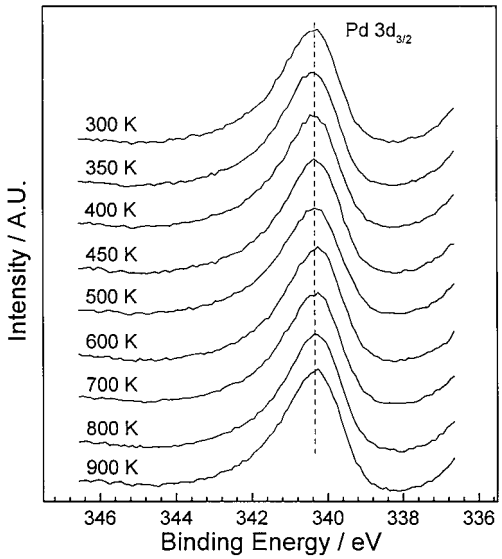

Figure 6. Annealing temperature effect on the Pd $3d_{3/2}$ peaks for 1 ML Cu/Pd(111).

reported for other Cu−Pd systems such as Cu/Pd/Mo(110) (350 K)[33] and Cu/Pd/mica (500 K).[34]

Figure 6 illustrates the effect of annealing temperature on the Pd $3d_{3/2}$ photoemission feature for the same 1.0 ML Cu/Pd(111) system discussed above. No significant shift in the Pd $3d_{3/2}$ binding energy as a function of annealing temperature was observed. The effect of annealing temperature on 0.5 ML Cu/Pd(111) was also investigated, and these results were qualitatively similar to those of 1.0 ML Cu/Pd(111).

4. Discussion

Layer-by-layer growth was observed for at least the first two Cu layers, agreeing well with the growth mode predicted on the basis of energetic considerations. Cu thin films on other open surfaces such as Pd(100)[21] and Pd(110)[22] also grow layer-by-layer. A previously reported LEED intensity analysis for Cu/Pd(111)[19] found no evidence of formation of a first complete layer, therefore excluding layer-by-layer growth in favor of Volmer−Weber growth. The results reported here based on the Cu $2p_{3/2}$ intensities and core-level shifts clearly indicate layer-by-layer growth, in contrast to the conclusions of ref 19, but consistent with other reported studies of Cu deposition on Pd surfaces.

To compare the core-level binding energy of the Cu monolayer with that of the multilayer, it is necessary to correct the superposition of the surface core-level shift with the bulk core-levels in the multilayer spectra. For example, for Cu coverages in excess of 1 ML, the XPS spectra are a convolution of electrons emitted from surface and subsurface Cu layers. Following the analysis methods of Rodriguez and Goodman,[31] the present results are summarized in Figure 7. The Cu $2p_{3/2}$ binding energy of the surface atoms from Cu(100) is known to be 0.22 eV lower than that of bulk Cu.[35] If the Cu $2p_{3/2}$ binding energy value from 20 ML Cu/Pd(111) is referenced to that of Cu(100) (also a combination of the surface and bulk), then a −0.64 eV core-level shift is observed for 1 ML Cu/Pd(111), which agrees well with the reported CLS for 1.0 ML Cu/10 ML Pd/Mo(110).[33] Furthermore, the core-level shift for 1 ML Cu/Pd(111) compared to the core-level shift from the surface layer of Cu(100) is −0.47 eV, similar to other experimental results (−0.38 eV) for 1 ML Cu/10 ML Pd/Mo(110)[33] and theoretical calculation results (−0.67 eV) for 1 ML Cu/

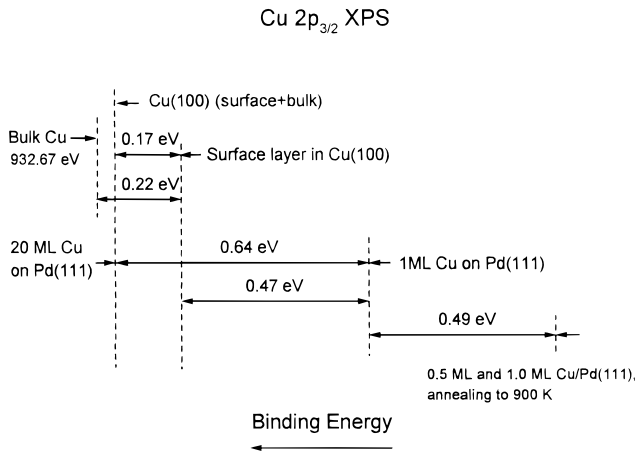

Figure 7. Relative Cu $2p_{3/2}$ XPS binding energies of bulk Cu, the surface atoms of Cu(100), a monolayer Cu on Pd(111), multilayer Cu on Pd, and 1.0 ML Cu/Pd(111) annealed to 900 K.

Pd(111).[36] The present data regarding annealing temperature effects show that upon annealing to 900 K, the Cu $2p_{3/2}$ peaks for 0.5 ML Cu/Pd(111) and 1 ML Cu/Pd(111) shift −0.49 eV. After annealing, the total shift for Cu $2p_{3/2}$ core levels from surface atoms in Cu(100) is −0.96 eV, again similar to −0.97 eV for Cu $2p_{3/2}$ in 1.0 ML Cu/10 ML Pd/Mo(110)[33] and −0.77 eV in bulk Cu−Pd alloys with dilute Cu (about 10%).[28]

It is well-known that overlayer clustering upon annealing can lead to negative core-level shifts due to exposure of a large portion of the second monolayer.[31,37] In general, with increasing overlayer thickness, the degree of clustering increases and the temperature onset of clustering decreases. In the cases of Cu/Ru(0001) and Cu/Rh(100),[31] the Cu core-level shift decreases upon annealing for coverages larger than 1 ML and can be attributed to Cu cluster formation on the refractory substrates. In contrast, a system like Pd/Au(111)[37] exhibits no Pd XPS peak shifts as a function of annealing temperature, so the possibility of clustering is excluded in favor of alloy formation. In the present experiments, the heat of mixing for CuPd is negative (−14 kJ mol^{-1}), with a dilute limit value of −62 kJ mol^{-1}.[18] Furthermore, the annealing experiments were carried out in the submonolayer regime, so it is unlikely that the Cu overlayer undergoes extensive clustering. Thus, with increasing temperature, intermixing occurs between Cu and Pd and a surface alloy is formed at intermediate temperatures. At higher temperatures, the surface and subsurface Cu apparently diffuses into the sample bulk.

These data clearly illustrate that a Cu overlayer supported on Pd(111) is electronically perturbed with respect to the surface layer of Cu(100) and that Cu−Pd alloying enhances this interaction. Several possible reasons exist for core-level shifts in mixed metal systems based on the homonuclear Cu−Cu bond and heteronuclear Cu−Pd bond interactions. The following discussion will focus on the different geometric and electronic perturbations that can give rise to the electronic property changes observed for Cu overlayers on Pd(111).

Geometric contributions to core-level shifts are related to the relative coordination of an overlayer with respect to a reference surface layer. For example, a Cu monolayer on Rh(100)[31] was found to grow pseudomorphically with a somewhat smaller (∼10%) surface atomic density than Cu(100). This result implies that the effective coordination of a Cu monolayer on Rh(100) is less than the coordination of Cu(100) surface atoms. It is generally observed that surfaces with lower coordination numbers have lower surface XPS binding energies. Thus, the reduction of the effective coordination of Cu/Rh(100) leads to a decrease in Cu $2p_{3/2}$ binding energy in part with respect to the surface atoms of Cu(100).

It has been reported that Cu grows pseudomorphically on Pd(111),[23] Pd(110),[22] Pd(100),[38] and Pt(111).[39] Therefore, Cu adopts the geometric lattice constant of the Pd(111) surface, yielding a Cu surface density that is very similar to that of Pd(111) ($\sim 1.5 \times 10^{15}$ atoms cm^{-2}). Furthermore, this surface density is approximately equal to the surface atomic density of Cu(100)($\sim 1.5 \times 10^{15}$ atoms cm^{-2}), implying that the effective coordination (in plane) of Cu in the Pd(111) surface is likely very similar to that of a Cu(100) surface. The overlayer Cu−Cu bonding then should be comparable to a Cu(100) surface layer, thus geometric contributions to the core-level shift should be negligible. Cu−Pd bonding then is likely the dominant factor leading to the observed core-level shifts.

Strong electronic interactions related to heterometallic Cu−Pd bond formation between the overlayer and the substrate may also substantially influence the core-level shifts. Rodriguez and Goodman[1,2,3] proposed that the core-level shift is mainly related to charge transfer between dissimilar metal overlayers. Although the bulk electronegativity of Cu (1.8) is smaller than Pd (2.0), Cu has a 4s conduction band that is only half occupied, while Pd has an essentially full valence band. Consequently, the formation of a heteronuclear metal−metal bond between Cu and Pd induces a flow of electron density from Pd to Cu. This behavior has also been observed for bulk Cu−Pd alloys[27,28] where interatomic charge transfer occurs from Pd to Cu. Thus, initial state charge transfer can play a significant role in determining the observed core-level shift. Similarly, it has been found that a monolayer of Cu on other late transition metal surfaces, such as Ru(0001), Pt(111), and Rh(100), probably accepts electrons from the substrate and that the magnitude of the SCLS increases with the filling of the substrate d band.[1,2,3]

Another effect that can contribute to core-level shifts is metal−metal bonding induced orbital rehybridization (polarization).[36,40,41] This hybridization is involved in deeper-lying valence levels in the local chemical bonding between neighboring atoms. For Cu, this would consist of hybridization and intra-atomic charge polarization of Cu 3d → Cu 4sp. For 1 ML Cu/Pd(111),[36] density functional theory calculations show that there is a noticeable internal polarization of the adlayer Cu atoms. The adsorption of Cu on Pd empties and shifts the surface Cu 3d density of states (DOS) toward the Fermi level. Consequently, the core electron levels shift toward the Fermi level as well, corresponding to a shift to lower binding energy.

The previously discussed effects on core-level shifts, namely charge transfer between dissimilar metals and orbital rehybridization, are both examples of initial state effects. However, final state effects are also often important factors in core-level shifts. As surface Cu atoms intermix with the Pd surface upon annealing, chemical environmental factors such as interatomic spacing, number of nearest neighbors, and types of nearest neighbors will certainly be altered. Therefore, in addition to initial state effects, final state screening effects can also become significant. Density functional calculations[25] show that for noble metal core levels, such as the Cu 2p levels in the random surface alloy $Pd_{1-x}Cu_x$/Cu(001), final state screening effects (including interatomic and intra-atomic screening) are significant. In addition, core-level shifts calculated for 1 ML Cu/Pd(111)[36] indicate that the screening contribution to Cu 2p core-level shifts is +0.17 eV, which partially cancels the initial-state contribution of −0.84 eV to yield an overall core-level shift of −0.67 eV, relative to a Cu(100) surface. In the present context, the core-

level shifts measured for $Pd_{1-x}Cu_x$/Pd(111) alloys almost certainly contain final state contributions.

For both Pd $3d_{3/2}$ and Pd(M_5VV), the binding energies do not shift upon alloy formation as significantly as the Cu $2p_{3/2}$ features. Density-functional theory calculations[25] suggest that for the random surface alloy $Cu_{1-x}Pd_x$/Pd(001), the Pd $3d_{3/2}$ feature exhibits at most a -0.05 eV shift at $x = 0.5$ and a $+0.10$ eV shift as $x \rightarrow 0$, compared with the top layer of Pd(001) due to the cancellation of the initial and final state effects. As for the present experimental data, the XPS signals are integrated over several top layers rather than just the top Pd layer, thus these thermally synthesized surface alloys are not true bulk Cu−Pd alloys. Within experimental error, the Pd $3d_{3/2}$ feature for Cu/Pd(111) is unchanged from Pd(111).

The precise contributions of initial and final state effects on the experimentally observed core-level shifts are still not fully understood; however, both must be considered when analyzing core-level shifts. Further experimental and theoretical work is essential for a more complete understanding of metal overlayer and alloy core-level binding energy shifts.

5. Conclusions

By employing XPS, the interaction between Cu thin films and Pd(111) was addressed. At room temperature, Cu grows layer-by-layer at least up to the first two atomic layers. The overlayer electronic structure is perturbed for 2−3 layers of Cu as seen by monitoring the core-level shifts. The Cu $2p_{3/2}$ binding energy of one Cu layer on Pd(111) is -0.47 eV lower than the surface atoms of Cu(100). Upon annealing to temperatures greater than 450 K, submonolayer coverages of Cu alloy with the Pd(111) surface. After annealing to 900 K, the Cu $2p_{3/2}$ binding energy shift is -0.49 eV relative to that of 1 ML Cu/Pd(111). No significant Pd $3d_{3/2}$ binding energy shifts were observed for annealing between 300 and 900 K. The observed core-level shifts are interpreted in terms of initial and final state contributions.

Acknowledgment. We acknowledge with pleasure the support of this work by the Department of Energy, Office of Basic Energy Sciences, Division of Chemical Sciences and the Amoco Corporation. In addition, P. S. Bagus is acknowledged for helpful discussions.

References and Notes

(1) Rodriguez, J. A.; Goodman, D. W. *Science* **1992**, *257*, 897 and references therein.
(2) Goodman, D. W. *J. Phys. Chem.* **1996**, *100*, 13090.
(3) Rodriguez, J. A. *Surf. Sci. Rep.* **1996**, *24*, 223.
(4) Campbell, C. T. *Annu. Rev. Phys. Chem.* **1990**, *41*, 775.
(5) Sinfelt, J. H. *Bimetallic Catalysts*; Wiley: New York, 1983.
(6) Choi, K. I.; Vannice, M. A. *J. Catal*. **1991**, 131, 36.
(7) Espeel, P. H.; De Peuter, G.; Tielen, M. C.; Jacobs, P. A. *J. Phys. Chem.* **1994**, *98*, 11588.
(8) Anderson, J. A.; Fernández-García, M.; Haller, G. L. *J. Catal*. **1996**, *164*, 477.
(9) Leon y Leon, C. A.; Vannice, M. A. *Appl. Catal.* **1991**, *69*, 305.
(10) Lianos, L.; Debauge, Y.; Massardier, J.; Jugnet, Y.; Bertolini, J. C. *Catal. Lett.* **1997**, *44*, 211.
(11) Skoda, F.; Astier, M. P.; Pajonk, G. M.; Primet, M. *Catal. Lett.* **1994**, *29*, 159.
(12) Nieuwenhuys, B. E. *Surf. Rev. Lett.* **1996**, *3*, 1869 and references therein.
(13) Dumas, P.; Suhren, M.; Chabal, Y. J.; Hirschmugl, C. J.; Williams, G. P. *Surf. Sci.* **1997**, *371*, 200 and references therein.
(14) DeBoer, F. R.; Boom, R.; Mattens, W. C. M.; Miedema, A. R.; Niessen, A. K. *Cohesion in Metals: Transition Metal Alloys*; DeBoer, F. R., Pettifor, D. G., Eds.; Elsevier: Amsterdam, 1988.
(15) Murray, P. W.; Stensgaard, I.; Lægsgaard, E.; Besenbacher, F. *Phys. Rev. B* **1995**, *52*, R14404.
(16) Murray, P. W.; Thorshaug, S.; Stensgaard, I.; Besenbacher, F.; Lægsgaard, E.; Ruban, A. V.; Jacobsen, K. W.; Kopidakis, G.; Skriver, H. L. *Phys. Rev. B* **1997**, *55*, 1380.
(17) Aaen, A. B.; Lægsgaard, E.; Ruban, A. V.; Stensgaard, I. *Surf. Sci.* **1998**, *408*, 43.
(18) Pope, T. D.; Griffiths, K.; Norton, P. R. *Surf. Sci.* **1994**, *306*, 294.
(19) Li, H.; Tian, D.; Jona, F.; Marcus, P. M. *Solid State Commun.* **1991**, *77*, 651.
(20) Kittel, C. *Introduction to Solid State Physics*; Wiley: New York, 1986; p 24.
(21) Hahn, E.; Kampshoff, E.; Wälchli, N.; Kern, K. *Phys. Rev. Lett.* **1995**, *74*, 1803.
(22) (a) Barnes, C.; Gleeson, M. *Surf. Sci.* **1994**, *319*, 157. (b) Hahn, E.; Kampshoff, E.; Fricke, A.; Bucher, J-P.; Kern, K. *Surf. Sci.* **1994**, *319*, 277.
(23) Oral, B.; Kothari, R.; Vook, R. W. *J. Vac. Sci. Technol.* A **1989**, *7*, 2020.
(24) Fernández-García, M.; Conesa, J. C.; Clotet, A.; Ricart, J. M.; López, N.; Illas, F. *J. Phys. Chem. B* **1998**, *102*, 141.
(25) Ganduglia-Pirovano, M. V.; Kudrnovský, J.; Scheffler, M. *Phys. Rev. Lett.* **1997**, *78*, 1807.
(26) Kucherenko, Y.; Perlov, A. Y.; Yaresko, A. N.; Antonov, V. N. *Phys. Rev. B* **1998**, *57*, 3844.
(27) Cole, R. J.; Brooks, N. J.; Weightman, P. *Phys. Rev. B* **1997**, *56*, 12178.
(28) Cho, En-Jin; Lee, S.; Oh, S.-J.; Han, M.; Lee, Y. S.; Whang, C. N. *Phys. Rev. B* **1995**, *52*, 16443.
(29) Parmeter, J. E.; Jiang, X.; Goodman, D. W. *Surf. Sci.* **1990**, *240*, 85.
(30) Beutler, A.; Strisland, F.; Sandell, A.; Jaworowski, A. J.; Nyholm, R.; Wiklund, M.; Andersen, J. N. *Surf. Sci*. **1998**, *411*, 111.
(31) Rodriguez, J. A.; Campbell, R. A.; Goodman, D. W. *J. Phys. Chem.* **1991**, *95*, 2477.
(32) Shek, M. L.; Stefan, P. M.; Lindau, I.; Spicer, W. E. *Phys. Rev. B* **1983**, *27*, 7277.
(33) Rainer, D. R.; Corneille, J. S.; Goodman, D. W. *J. Vac. Sci. Technol. A* **1995**, *13*, 1595.
(34) Vook, R. W.; Bucci, J. V.; Chao, S. S. *Thin Solid Films* **1988**, *163*, 447.
(35) Egelhoff, W. F. *Phys. Rev. B* **1984**, *29*, 4769.
(36) Hennig, D.; Ganduglia-Pirovano, M. V.; Scheffler, M. *Phys. Rev. B* **1996**, *53*, 10344.
(37) Koel, B. E.; Sellidj, A.; Paffett, M. T. *Phys. Rev. B* **1992**, *46*, 7846.
(38) Li, H.; Wu, S. C.; Tian, D.; Quinn, J.; Li, Y. S.; Jona, F.; Marus, P. M. *Phys. Rev. B* **1991**, *44*, 8261.
(39) Ibach, H.; Erley, W.; Wagner, H. *Surf. Sci.* **1980**, *92*, 29.
(40) Bagus, P. S.; Brundle, C. R.; Pacchioni, G.; Parmigiani, F. *Surf. Sci. Rep.* **1993**, *19*, 265.
(41) Rodriguez, J. A.; Goodman, D. W. *Acc. Chem. Res.* **1995**, *28*, 477.